

Artificial Immune Based Medical Image Classification by Optimized Features and Ensemble Tree Learning Model

Surendra Singh Vishwakarma¹, Dr Vijay Bhandari², Dr Praneet Saurabh³

¹Research Scholar, Department of Computer Science and Engineering Madhyanchal Professional University Bhopal, M.P, India

²Professor, Department of Computer Science and Engineering Madhyanchal Professional University Bhopal, M.P, India

³Professor, Department of Computer Science and Engineering Manipal University Jaipur, Rajasthan, India.

Abstract- Skin cancer poses a serious threat to human health worldwide, affecting a large number of individuals. Therefore, early detection and accurate diagnosis are crucial, and dermoscopic imaging plays a vital role in identifying these conditions at an initial stage. This paper has proposed a model that classify the skin medical image into healthy and non-healthy image. Whole model is divide into two module first improve the input image data quality by removing noise and identifying the effecting portion of image that impact more. Further second module extract the histogram and CCM features from the image to train the Ensemble Tree model. Experiment is done on real dataset of skin cancer images. Result shows that proposed MICAIML (Medical Image Classification using Artificial Immune Machine Learning Model) has increase the detection accuracy by % as compared to existing model.

Keywords: Genetic algorithm, Image Processing, Feature Embedding, Extraction, Ensemble Learning.

I. INTRODUCTION

The term "skin cancer" (SC) describes a group of diseases in which abnormal skin cells grow uncontrollably and form tumors over time. The main factor responsible for this condition is prolonged exposure to ultraviolet (UV) radiation [1]. Skin cancer has become a serious global public health concern, significantly impacting human health and quality of life. It is one of the most commonly diagnosed forms of cancer worldwide [2]. According to the World Health Organisation (WHO), nearly one-third of all cancer cases are related to some form of skin cancer [3].

In addition to its high prevalence, the economic burden of skin cancer is considerable. Studies show that the annual cost of treating both melanoma and non-melanoma skin cancers in the United States exceeds eight billion dollars [4]. Beyond financial implications, patients undergoing treatments such as surgery, radiation therapy, or chemotherapy often experience substantial physical and psychological side effects [5]. Furthermore, visible scars and disfigurement caused by treatment can negatively

affect a patient's self-esteem and overall quality of life. Melanoma, the most aggressive and deadly type of skin cancer, can be fatal if not detected and treated at an early stage [5].

Dermoscopy is considered one of the most effective non-invasive techniques for identifying malignant, benign, and other pigmented skin lesions [6]. Traditionally, melanoma detection has relied on visual inspection, where clinicians examine changes in skin color and patterns with the naked eye. This conventional approach mainly focuses on surface features such as color variation and texture. However, dermoscopy enhances this process by providing a more detailed view of the skin, enabling improved classification of lesions based on their visual and structural characteristics [7]. In clinical practice, dermatologists often depend on their experience when interpreting dermoscopic images. Due to the subjective nature and complexity of such evaluations, computer-based analysis of dermoscopy images has gained significant attention as a way to reduce diagnostic errors [8].

To overcome these challenges, extensive research has been conducted on classifying malignant and benign skin cancers using automated image analysis techniques. These approaches integrate fields such as image processing, computer vision, and machine learning to perform tasks like lesion segmentation, detection, and melanoma classification [9]. Despite these advancements, limitations such as insufficient datasets and lack of diversity in skin lesion samples remain major concerns. Additionally, traditional diagnosis methods that rely solely on human judgment can lead to inconsistencies and inaccuracies.

Intelligent imaging-based systems for skin cancer detection have emerged as valuable tools to support physicians in clinical decision-making. Dermoscopy, as a non-invasive imaging method, plays a crucial role in this process by capturing magnified and well-illuminated images of affected skin areas. This enhanced visualization improves the clarity of skin lesions, facilitating more accurate diagnosis and analysis.

II. RELATED WORK

Wu et al. [10] introduced MHorUNet, an enhanced version of the UNet architecture designed specifically for accurate skin lesion segmentation. This model stands out due to its ability to capture high-order spatial interactions, allowing it to better understand complex contextual relationships within lesion regions. By integrating an attention mechanism, MHorUNet enhances segmentation performance and effectively refines the boundaries of lesions, particularly those with irregular or unclear edges. Experimental results on the ISIC dataset demonstrate that this model significantly outperforms traditional UNet-based approaches.

Lilhore et al. [11] proposed SkinEHDLF, a hybrid deep learning framework aimed at improving the diagnosis of skin cancer in complex scenarios. This approach combines conventional deep learning models with advanced feature extraction methods to achieve higher classification accuracy, particularly for challenging and diverse skin lesion types. The model was evaluated on a wide range of dermoscopic

images and was designed to handle variations in lesion appearance, thereby increasing diagnostic reliability. The findings highlight its potential for real-world clinical applications, where accurate skin cancer diagnosis remains challenging due to the diversity in lesion characteristics across different populations.

Al-Waisy et al. [12] proposed a comprehensive end-to-end deep learning framework for the early detection and classification of skin cancer lesions using dermoscopic images. Their approach employs advanced convolutional neural network (CNN) architectures to perform both segmentation and classification, enabling effective differentiation between malignant and benign lesions. The model incorporates multi-scale feature extraction techniques, which improve the localization of lesions, especially in cases where boundaries are unclear or contrast is low, such as in early-stage melanoma. Furthermore, the authors enhanced their framework with a more robust segmentation strategy and demonstrated that it outperforms existing state-of-the-art methods in terms of accuracy. These findings suggest that the proposed model holds strong potential as a reliable tool for early skin cancer diagnosis.

Firozi et al. [13] employed pre-trained deep learning models combined with fine-tuning to address domain-specific challenges in skin cancer analysis. While this approach achieved strong performance, it faced limitations such as class imbalance and a lack of interpretability.

Nunnari et al. [14] further investigated the consistency between Grad-CAM saliency maps and clinically relevant visual features. Their findings revealed noticeable mismatches, underscoring the need for more dependable and clinically meaningful explanation techniques. Although there has been encouraging progress, the comprehensive integration of explainable artificial intelligence (XAI) into dermatological cancer diagnosis is still at an early stage. Moreover, while the Swish activation function has shown effectiveness in general computer vision tasks, its adoption in dermatological

imaging remains limited, with most existing studies relying on ReLU or transfer learning approaches.

J. Musaev et al. [15] introduced IMed-CNN, an ensemble-based framework designed to enhance the accuracy of medical image classification. Their method begins with dataset preprocessing followed by training a customized model, from which the best-performing training stages are selected. To capture a wide range of image features, separate models are trained on individual RGB channels as well as different pixel intensity levels. A structured dropout mechanism is then applied to eliminate less effective models, while Unique True Prediction (UTP) analysis is used to retain models that provide distinct and accurate predictions. During the testing phase, outputs from the selected models are combined using a weighted strategy, resulting in a more robust and reliable classification system.

III. PROPOSED METHODOLOGY

Paper has proposed a model term as MICAIML (Medical Image Classification using Artificial Immune Machine Learning Model) for medical image classification. Fig. 1 shows two modules of work where first shows the image feature optimization and second module for training the mathematical model. Input image is pass from the first module that improve data quality by applying the artificial immune genetic operation. Further image features were extracted from the image. Extracted features were used for the training of the ENSEMBLE TREE model. Table 1 shows various notations used in the work for the explanation of model.

Input Raw Dataset

Input medical image raw dataset (MRD) is collection of images. Whole data is divide into two set first is training set and other is testing set. Each image class is known in the training and testing both set.

First Module

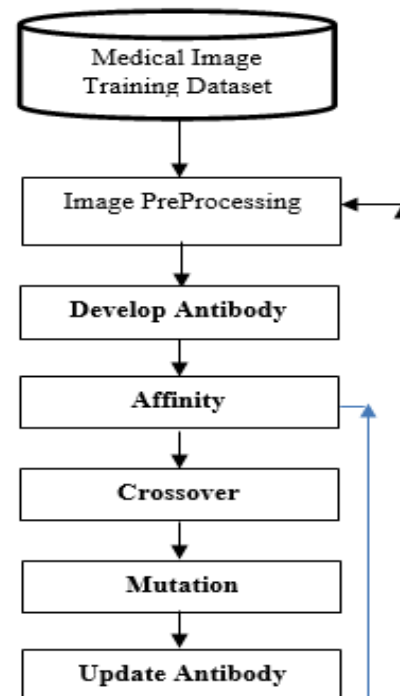
In this module image is preprocess first further image was filter and transformed into optimized image. Each input image I_i was taken from MRD is treated and optimize in this module.

Table 1 Notation used in MICWSN.

Notation	Meaning
MRD	Medical Raw Dataset
P _i	Processed Image
A _p	Antibody Population
s	Number of segment
b	Number of antibody in Population
A _f	Affinity Value
I	Image Matrix
i	Matrix x position
j	Matrix y position
A _P I	Artificial Processed Image
E _f	Extracted Feature
TETM	Trained ETM

Pre-Processing: MRD training set of I_i is transform into required matrix dimension. Further image is filter to reduce the noise. Median filter was used in the work for the image noise removal. P_i image need to be process into gray scale to identify the effecting feature set.

$P_i \leftarrow \text{Raw_Image_Processing}(\text{MRD})$



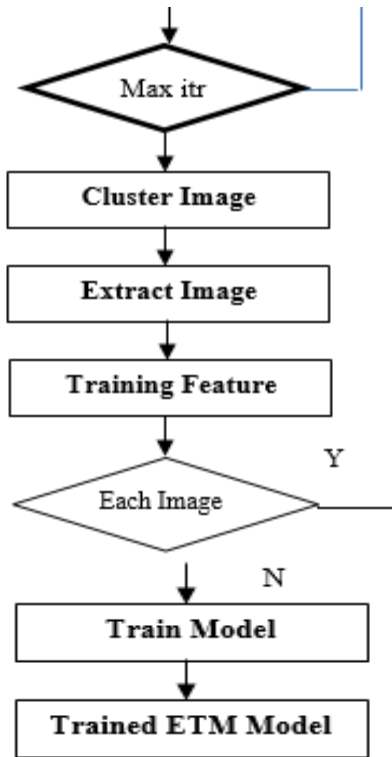


Fig. 1 Block diagram of proposed MICAIML model.

Artificial Immune Genetic Algorithm

Processed image is segment into two part that identify the affecting and non affecting feature set of image. This work has implement the artificial immune genetic algorithm for the image segment [16]. Few of common steps of the model is to generate various segment center sets know as antibodies, further get the fitness of each segment center set and as per fitness crossover, mutation operation are important modification steps of algorithm.

$$A_p \leftarrow \text{Antibody_Population}(P_i, s, b)$$

Generate Antibody: In order to identify the segment center random set of pixel values were taken as segment center set in the algorithm. Each set of segment center is term as antibody. Collection of antibodies is population. Algorithm gather s number of pixels and b number of antibodies in the population.

Affinity: Each antibody have its affinity value for the pixel segmentation. Paper has evaluate the affinity by estimating the pixel diferece from its segment

center pixel values. Sum of each difference value is term as affinity. Affinity value of lower pixel value antibody set is good for the work. Lower difference value give better pixel segment pixel set.

$$A_f \leftarrow \text{Affinity}(A_p, P_i)$$

Crossover: Getting the better solution is the ultimate goal of the genetic algorithm hence most of algorithm do by crossover and mutation. Artificial immune uses both. In crossover work this work sort the affinity value and perform the crossover best with worst, then next best with next worst antibody. This help to get the better solution if new child antibody affinity value is better than parent one. In this step selected two antibody go under crossover where good affinity value antibody modify the segment pixel set of other antibody in crossover.

$$A_p \leftarrow \text{Antibody_Crossover}(A_f, A_p)$$

Mutation: In this population modification step algorithm itself replace the pixel value by random other pixel value and create a new child antibody. Work has got new set of antibodies in this step as well. Hence population need to be clear with high affinity antibodies.

$$A_p \leftarrow \text{Antibody_Mutation}(A_p)$$

Update Antibody: Each child antibody affinity value is compared with its parent one and low affinity value antibody is removed from the population. After this algorithm repeat above steps for fix number of t iterations.

$$A_p \leftarrow \text{Update_Population}(A_p)$$

Final A_p best affinity antibody is selected as the fitness segment of the image. Work segment the pixel into affecting and non-affecting segment. Affecting segment of image is used for the feature extation in second module.

$$A_{PI} \leftarrow \text{Segment}(P_i, A_f)$$

Second Module

Extract Features: This work extract co-occurrence matrix features and histogram feature from the affecting segment of image. In histogram sixteen bins of gray scale image features were used, so each image gives 16 feature value. Futher paper extract CCM feature that transfored the image into RGB

(Red Green, Blue) and HSV (Hue Saturation Value) format.

To analyze the texture characteristics of an image, one of the most important techniques used is the co-occurrence matrix. This method captures texture information by examining the spatial relationship between neighboring pixels. It provides a quantitative description of the image's surface properties, making it highly useful for feature extraction. In this study, four key texture features are considered: contrast, energy, inverse difference, and entropy, each of which contributes to a better representation of the underlying surface patterns [17].

$$ID = \sum_{i=1} \sum_{j=1} \frac{1}{(1 + (i - j)^2)} I(i, j)$$

$$Entropy = -\sum_{i=1} \sum_{j=1} I(i, j) \log[I(i, j)]$$

$$Energy = \sum_{i=1} \sum_{j=1} (I(i, j))^2$$

$$Contrast = \sum_{i=1} \sum_{j=1} (i - j)^2 * I(i, j)$$

Extracted CCM features for four matrix of Red, Green, Hue and Saturation was collect so total 16 values were collect form the CCM as well. This work is need to normalize the CCM features.

$$Ef \leftarrow \text{Extract_HIST_CCM}(API)$$

Train Ensemble Model

Training a bagger tree learning model for skin cancer image classification follows a systematic pipeline that begins with collecting a dermoscopic image dataset and performing preprocessing steps such as resizing images to a uniform size, normalizing pixel intensities, and applying augmentation techniques like rotation, flipping, and scaling to improve generalization [18]. After preprocessing, meaningful features are extracted from the images, such as texture, color, and statistical properties, which serve as input for the learning model. These extracted features are then used to train a bagging-based decision tree model, where multiple decision trees

are generated using different subsets of the training data through bootstrap sampling. Each tree learns distinct patterns from the dataset, reducing variance and improving robustness. During classification, predictions from all trees are combined using a majority voting mechanism to produce the final output. This ensemble approach enhances classification accuracy and stability, making it effective for reliable skin cancer detection.

$$TETM \leftarrow \text{Train_ETM}(Ef)$$

Proposed MICAIML Algorithm

Input: MRD

Output: TETM

1. Loop 1:n // n number of training image
2. Pli•Raw_Image_Processing(MRD)
3. Ap•Antibody_Population(Pli, s, b)
4. Loop it // t number of iteration
5. Af•Affinity(Ap, PI)
6. Ap•Antibody_Crossover(Af, Ap)
7. Ap•Antibody_Mutation(Ap)
8. Ap•Update_Population(Ap)
9. EndLoop
10. API•Segment(PI, Af)
11. Ef•Extract_HIST_CCM(API)
12. TETM•Train_ETM(Ef)

The proposed MICAIML algorithm begins by preprocessing the input MRD images to obtain refined representations suitable for analysis. An antibody population is then generated and iteratively optimized through affinity evaluation, crossover, mutation, and population updating to enhance feature selection. After optimization, the segmented image is produced and relevant features are extracted using histogram and co-occurrence matrix techniques. Finally, these extracted features are used to train the TETM model for accurate classification of skin cancer images.

IV. EXPERIMENT AND RESULTS

The model was implemented using MATLAB 2016a. All experiments were carried out on a system equipped with a 12th generation Intel i3 processor and 8 GB of RAM. Comparison of proposed MICWSN

model was done with existing model proposed in [15]. Experiment was done real medical images taken from [19]. Table 2 shows experimental data images.

Results

Table 2 presents the comparison of precision values between IMEDCNN [10] and the proposed MICAIML approach across different dataset sizes. It can be observed that MICAIML consistently outperforms IMEDCNN for all testing samples, achieving perfect precision (1.0) at 60 images and maintaining higher values as the dataset increases. On average, MICAIML shows an improvement of approximately 22.14% in precision over IMEDCNN, indicating its superior capability in correctly identifying positive cases while minimizing false positives.

Table 2 Medical Image Classification models comparison on the basis of precision values.

Testing Dataset	IMEDCNN [10]	MICAIML
60	0.8077	1
120	0.6863	0.8197
180	0.6703	0.8478
240	0.6612	0.8843
300	0.641	0.9007

Table 3 Medical Image Classification models comparison on the basis of recall values.

Testing Dataset	IMEDCNN [10]	MICAIML
60	0.7	0.9375
120	0.6481	0.8197
180	0.6489	0.8667
240	0.645	0.877
300	0.6452	0.8889

Table 4 illustrates the recall performance of both models, highlighting the ability to correctly detect actual positive instances. The MICAIML method demonstrates significantly higher recall values compared to IMEDCNN, especially for smaller datasets where it reaches 0.9375. Even with increasing dataset size, MICAIML maintains consistent performance, resulting in an average improvement of about 25.11% over the existing model. This confirms its effectiveness in reducing false negatives and improving detection sensitivity.

Table 4 Medical Image Classification models comparison on the basis of f-measure values.

Testing Dataset	IMEDCNN [10]	MICAIML
60	0.75	0.9677
120	0.6667	0.8197
180	0.6489	0.8571
240	0.6531	0.8807
300	0.6431	0.8947

Table 5 compares the F-measure values, which provide a balanced evaluation of both precision and recall. The proposed MICAIML model achieves notably higher F-measure scores across all dataset sizes, reflecting its balanced and reliable classification performance. The average improvement observed is 23.93%, demonstrating that MICAIML effectively maintains both high precision and recall simultaneously, unlike IMEDCNN which shows comparatively lower and less stable values.

Table 5 Medical Image Classification models comparison on the basis of accuracy values.

Testing Dataset	IMEDCNN [10]	MICAIML
60	72	96.6667
120	65	81.9672
180	63.33	85.9459
240	64.58	88.0165
300	63.6066	89.8089

Table 5 shows the accuracy comparison between the two models. The MICAIML approach significantly enhances classification accuracy, achieving up to 96.66% for smaller datasets and consistently higher performance for larger datasets as well. On average, the proposed method improves accuracy by approximately 25.74% compared to IMEDCNN. This substantial gain highlights the robustness and overall effectiveness of MICAIML in medical image classification tasks.

V. CONCLUSION

In conclusion, this paper presented the MICAIML (Medical Image Classification using Artificial Immune Machine Learning) model as an effective approach

for skin cancer image classification. The proposed method integrates artificial immune genetic operations for feature optimization with an ensemble tree-based learning model for accurate classification. The first module enhances image quality through preprocessing, segmentation, and optimized antibody-based feature selection, while the second module focuses on extracting meaningful histogram and co-occurrence matrix features. These features are then utilized to train a robust ensemble tree model. Experimental results demonstrate that MICAIML significantly outperforms existing methods in terms of precision, recall, F-measure, and accuracy, achieving average improvements of over 20% across all metrics. The model shows strong capability in handling complex image patterns and reducing misclassification. Overall, MICAIML provides a reliable, efficient, and scalable solution for medical image analysis, making it highly suitable for real-world skin cancer diagnosis applications.

REFERENCES

1. D.N. Dorrell et al. Skin cancer detection technology *Dermatol. Clin.* (2019)
2. O. Attallah RADIC: a tool for diagnosing COVID-19 from chest CT and X-ray scans using deep learning and quad-radiomics *Chemometr. Intell. Lab. Syst.* (2023)
3. R.C. Maron et al. Robustness of convolutional neural networks in recognition of pigmented skin lesions *Eur. J. Cancer* (2021)
4. O. Attallah CerCan• net: cervical cancer classification model via multi-layer feature ensembles of lightweight CNNs and transfer learning *Expert Syst. Appl.* (2023)
5. R. Karthik et al. Classification of breast cancer from histopathology images using an ensemble of deep multiscale networks *Biocybern. Biomed. Eng.* (2022)
6. Zghal N.S., Derbel N. Melanoma Skin Cancer Detection based on Image Processing. *Curr. Med. Imaging.* 2020;16:50–58.
7. Polat K., Koc K.O. Detection of skin diseases from dermoscopy image using the combination of convolutional neural network and one-versus-all. *J. Artif. Intell. Syst.* 2020;2:80–97.
8. Wei L., Ding K., Hu H. Automatic Skin Cancer Detection in Dermoscopy Images based on Ensemble Lightweight Deep Learning Network. *IEEE Access.* 2020;8:99633–99647.
9. Ech-Cherif A., Misbhauddin M., Ech-Cherif M. Deep Neural Network-based mobile dermoscopy application for triaging skin cancer detection; *Proceedings of the 2019 2nd International Conference on Computer Applications & Information Security (ICCAIS); Riyadh, Saudi Arabia. 1–3 May 2019.*
10. Wu, R. et al. MHorUNet: High-order Spatial interaction UNet for skin lesion segmentation. *Biomed. Signal Process. Control.* 88, 105517.
11. Lilhore, U. K. et al. SkinEHDLF a hybrid deep learning approach for accurate skin cancer classification in complex systems. *Sci. Rep.* 15, 14913 (2025).
12. Al-Waisy, A. S. et al. A deep learning framework for automated early diagnosis and classification of skin cancer lesions in dermoscopy images. *Sci. Rep.* 15, 31234 (2025).
13. Firozi D, Kumar D. Classification of Skin Cancer Detection using CNN. *Proceedings of the 2024 international conference on electrical electronics and computing technologies (ICEECT).* 2024; 1(1), 1–7. *IEEE.*
14. Nunnari F, Kadir MA, Sonntag D. On the overlap between grad-cam saliency maps and explainable visual features in skin cancer images. *International Cross-Domain Conference for Machine Learning and Knowledge Extraction.* 2021:241–53.
15. J. Musaev et al., "IMed-CNN: Ensemble Learning Approach With Systematic Model Dropout for Enhanced Medical Image Classification Using Image Channels and Pixel Intervals," in *IEEE Access*, vol. 13, pp. 138020-138036, 2025.
16. Oday A. Ahmed, K.H. Chong, S.P. Koh, Chong Tak Yaw, Jagadeesh Pasupuleti, Artificial immune systems (GA-AIS) enabled power loss mitigation in distributed generation: X3PAIS optimization approaches, *Heliyon*, Volume 10, Issue 18, 2024
17. Choirul Amin, Wahyu Tyas Pramono, Jumadi Jumadi, Dewi Novita Sari, Maxim G.M. Samson, Navigating urban poverty: The role of livelihood capital in the livelihood strategies of urban

- beggars in Indonesia, Social Sciences & Humanities Open, Volume 11, 2025,
18. Kotsiantis, S.B., Tsekouras, G.E., Pintelas, P.E. (2005). Bagging Model Trees for Classification Problems. In: Bozani, P., Houstis, E.N. (eds) Advances in Informatics. PCI 2005. Lecture Notes in Computer Science, vol 3746. Springer, Berlin, Heidelberg.
 19. <https://dataverse.harvard.edu/dataset.xhtml?persistentId=doi:10.7910/DVN/DBW86T>